

Chemical Science

Volume 12
Number 3
21 January 2021
Pages 817–1178

rsc.li/chemical-science



ISSN 2041-6539

EDGE ARTICLE

Amnon Bar-Shir *et al.*
Elucidating dissociation activation energies in host-guest
assemblies featuring fast exchange dynamics

Cite this: *Chem. Sci.*, 2021, 12, 865

All publication charges for this article have been paid for by the Royal Society of Chemistry

Elucidating dissociation activation energies in host–guest assemblies featuring fast exchange dynamics†

Ronit Shusterman-Krush,^a Laura Grimm,^b Liat Avram,^c Frank Biedermann^b and Amnon Bar-Shir^{*a}

The ability to mediate the kinetic properties and dissociation activation energies (E_a) of bound guests by controlling the characteristics of “supramolecular lids” in host–guest molecular systems is essential for both their design and performance. While the synthesis of such systems is well advanced, the experimental quantification of their kinetic parameters, particularly in systems experiencing fast association and dissociation dynamics, has been very difficult or impossible with the established methods at hand. Here, we demonstrate the utility of the NMR-based guest exchange saturation transfer (GEST) approach for quantifying the dissociation exchange rates (k_{out}) and activation energy ($E_{a,out}$) in host–guest systems featuring fast dissociation dynamics. Our assessment of the effect of different monovalent cations on the extracted $E_{a,out}$ in cucurbit[7]uril:guest systems with very fast k_{out} highlights their role as “supramolecular lids” in mediating a guest’s dissociation E_a . We envision that GEST could be further extended to study kinetic parameters in other supramolecular systems characterized by fast kinetic properties and to design novel switchable host–guest assemblies.

Received 14th October 2020
Accepted 1st December 2020

DOI: 10.1039/d0sc05666a

rsc.li/chemical-science

Introduction

For many supramolecular host–guest systems, elucidating their kinetic characteristics is critical for thoroughly understanding their performance and further improving their design as synthetic channels,¹ receptors,² transporters,³ drug carriers,⁴ catalysts,⁵ stimuli-responsive materials^{6,7} and more. Controlling the kinetic properties in such systems can be obtained through an external stimulus that changes the system’s activation energy (E_a) so as to yield an “open” or “closed” state of the host and, thus, govern the exchange dynamics of the bound guest. Considerable advances have been made in the design of such switchable open/closed molecular hosts and their response to a variety of external stimuli, such as pH,⁸ light,⁹ heat,¹⁰ redox¹¹ and more. However, a robust and accessible tool for studying their effect on the dissociation activation energy E_a ($E_{a,out}$) in a quantitative manner, which is crucial for the further development and improved performance of such systems, has yet to be offered. Indeed, well-established classical methods, such as

stopped-flow experiments,¹² UV-Vis measurements¹³ and exchange spectroscopy (EXSY)-NMR,¹⁴ are useful for characterizing slow dynamic processes. Nevertheless, these analytical tools are less favourable when it comes to supramolecular complexes with fast exchange dynamics, including the evaluation of such systems’ E_a values.

Applying the chemical exchange saturation transfer (CEST) NMR method to the study of host–guest systems using a hyperpolarized ^{129}Xe gas guest¹⁵ has opened new opportunities for quantifying exchange dynamics in supramolecular assemblies. Indeed, hyperCEST was applied to a wide array of molecular hosts, such as cryptophanes,^{16,17} cucurbit[n]urils (CB n),^{18–20} pillar[n]arenes²¹ and paramagnetic-capsules,²² demonstrating its applicability to a range of exchange regimes that are dependent on the host properties.²³ The combination of CEST and ^{19}F -NMR^{24,25} and its extension to host–guest systems^{26–28} have expanded the arsenal of molecular guests that are suitable for CEST-based studies beyond that of ^{129}Xe . This approach, termed guest exchange saturation transfer (GEST),²⁹ allows – as we introduce herein – now also the use of conventional NMR-setups to quantitatively study host–guest dissociation rates (k_{out}) and $E_{a,out}$. In fact, most host–guest systems that we are aware of display such low activation energies (and thus very fast complex formation and dissociation rate constants) that their study is simply infeasible by the available methods. In several cases, direct binding assays can be used in combination with stopped-flow experiments,^{30–34} particularly, when a chromophoric or emissive guest considerably alters their

^aDepartment of Organic Chemistry, Weizmann Institute of Science, Rehovot, 7610001, Israel. E-mail: amnon.barshir@weizmann.ac.il

^bInstitute of Nanotechnology (INT), Karlsruhe Institute of Technology (KIT), Hermann-von-Helmholtz Platz 1, 76344 Eggenstein-Leopoldshafen, Germany

^cDepartment of Chemical Research Support, Weizmann Institute of Science, Rehovot, 7610001, Israel

† Electronic supplementary information (ESI) available: For experimental details and supporting figures. See DOI: 10.1039/d0sc05666a

spectroscopic properties upon binding to the host. However, often in these cases a too fast complex formation is observed which is completed within the mixing time (“dead time”) of the technique. Thus, alternative methods for quantifying kinetic parameters applicable to the study of fast equilibrating host-guest systems are still in need.

We demonstrate here how the GEST-NMR method can be used to quantify relatively fast k_{out} values, which makes it complementary to other tools,^{35,36} including those based on NMR (*i.e.*, EXSY),³⁷ which are better suited for studying slow exchange rates. By exploring the relationship between k_{out} rates and the applied temperature, we demonstrate GEST's use as an analytical method for the study of $E_{\text{a,out}}$ in host-guest systems.

Specifically, we show that GEST-NMR can be used to quantitatively elucidate $E_{\text{a,out}}$ values of fluorinated guests (G) from cucurbit[7]uril (CB7). The CB7^{38–41} molecular host has a broad range of applications through host-guest inclusion complex formation,^{42–46} but also shows an unprecedented affinity to cations through ion-dipole interactions forming “supramolecular-lids”^{47–51} that mediate both thermodynamic⁵² and kinetic properties^{31,53,54} of CB7:G systems. Herein, we demonstrate the capability of GEST-NMR to quantify the effect of cationic-CB7 “lids” on the $E_{\text{a,out}}$ values of fast-exchanging guests, thus establishing it as an accessible analytical tool for future kinetic studies in supramolecular systems.

Results and discussion

In the here presented study, we characterized the following three host-guest systems regarding their k_{out} values by GEST-NMR: CB7 as host with halothane (G1), 5-fluorotryptophan (G2), and fluorene (G3) as guests (Fig. 1). As a first step, we acquired ¹⁹F-NMR spectra for each system to classify them roughly as either slow or fast exchanging on the NMR timescale (Fig. 2a and S1†). While CB7:G1 clearly exhibited the typical additional peak of a bound guest (upfield shifted to that of free G1), the spectra of CB7:G2 and CB7:G3 featured only a single peak, assigned to the non-bound guest. The clear, sharp, distinct peaks in the CB7:G1 spectrum are typical for a relatively slow exchange regime on the NMR timescale. However, faster exchange processes, as in the cases of CB7:G2 and CB7:G3 (Fig. 2a), lead to NMR-line broadening and peak coalescence,

which prevent one from distinguishing between free and bound guests in the ¹⁹F-NMR spectra.

To further elaborate on this observation, GEST experiments were carried out on solutions containing the studied CB7:G systems. When performing GEST-NMR experiments of a CB7:G1 complex at room temperature (298 K), a well-defined saturation transfer effect was observed at the frequency of the bound peak (Fig. 2a, left). Interestingly, in the equivalent GEST-NMR experiment of CB7:G2, we found a clear GEST effect (Fig. 2b, middle), marked by the lack of the characteristic CB7:G2 peak in the ¹⁹F-NMR spectrum (Fig. 2a, middle). In the CB7:G3 solution at 298 K, there was no observable asymmetry in the GEST-spectrum (Fig. 2b, right). Nonetheless, the isothermal titration calorimetry (ITC) experiments indicated the formation of CB7:G3 with an association constant K_{a} of $7 \times 10^4 \text{ M}^{-1}$ (Fig. S2†), which indicates a system with fast exchange kinetics that is accompanied by symmetric GEST spectrum (Fig. 2b, right).

In order to quantify the guest dissociation rates of each of the CB7:G systems, we set up a series of GEST experiments with varied pre-saturation pulses (B_1 , Fig. 2c). Fitting the experimental data to the Bloch-McConnell equations⁵⁵ allowed us to quantitatively evaluate the k_{out} of the studied CB7:G systems. As expected, CB7:G1 (Fig. 2, left) exhibited relatively slow dissociation kinetics, with $k_{\text{out}} = 15 \pm 1 \text{ s}^{-1}$; this k_{out} value fits in the slow exchange rate regime on the NMR timescale, with a $k_{\text{out}} \ll \Delta\omega$ for a $\Delta\omega$ of 1.3 ppm (equal to 490 Hz at 9.4 T NMR) offset between free and bound G1 in the ¹⁹F-NMR spectrum. Note that such a slow k_{out} value could also be quantified with the established EXSY-NMR method,⁵⁶ which, as noted above, is not applicable to host-guest systems with faster dissociation rates where two distinct NMR peaks are not detected (as shown for G2 and G3 in Fig. 2). Ideally suited for the study of faster exchange regimes,⁵⁷ GEST-NMR was used to quantify the k_{out} of CB7:G2, found to be $2000 \pm 100 \text{ s}^{-1}$ (for $\Delta\omega$ of $\sim 1200 \text{ Hz}$; Fig. 2c, middle). Nevertheless, we were unable to determine the exchange rate by which G3 is excluded from its CB7:G3 complex ($k_{\text{out}} > 4000 \text{ s}^{-1}$, 298 K, Fig. 2c, right), as a very broad z-spectrum was obtained (Fig. 2b, right). Thus, we can use GEST-NMR to differentiate between the kinetic regimes of each of the above-mentioned host-guest systems – CB7:G1, CB7:G2 and CB7:G3, representing slow-, intermediate-, and fast-exchange processes on the NMR timescale at room temperature (298 K), respectively.

For the elucidation of the binding mechanism, and thus for obtaining deeper insights into non-covalent interactions and supramolecular principles, the knowledge of the activation energies is of utmost benefit.

Having identified two CB7:G systems that experience intermediate-to-fast k_{out} rates ($>2000 \text{ s}^{-1}$), we turned to evaluate the capability of GEST-NMR to determine the $E_{\text{a,out}}$. To this end, the k_{out} values for both CB7:G2 and CB7:G3 were determined at a series of temperatures and then correlated to the inverse temperature using the Arrhenius equation (eqn (1)):

$$\ln(k_{\text{out}}) = \frac{-E_{\text{a,out}}}{R} \left(\frac{1}{T} \right) + \ln(A) \quad (1)$$

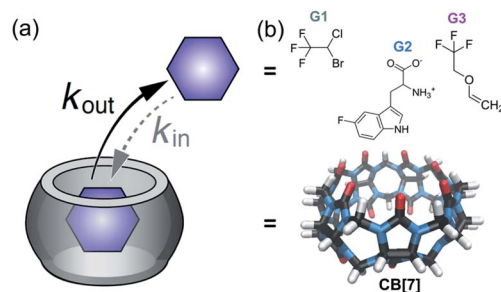


Fig. 1 Dynamic CB7:guest systems. (a) Schematic representation of the studied dynamic process. (b) Chemical structures of CB7 and guests G1–G3.



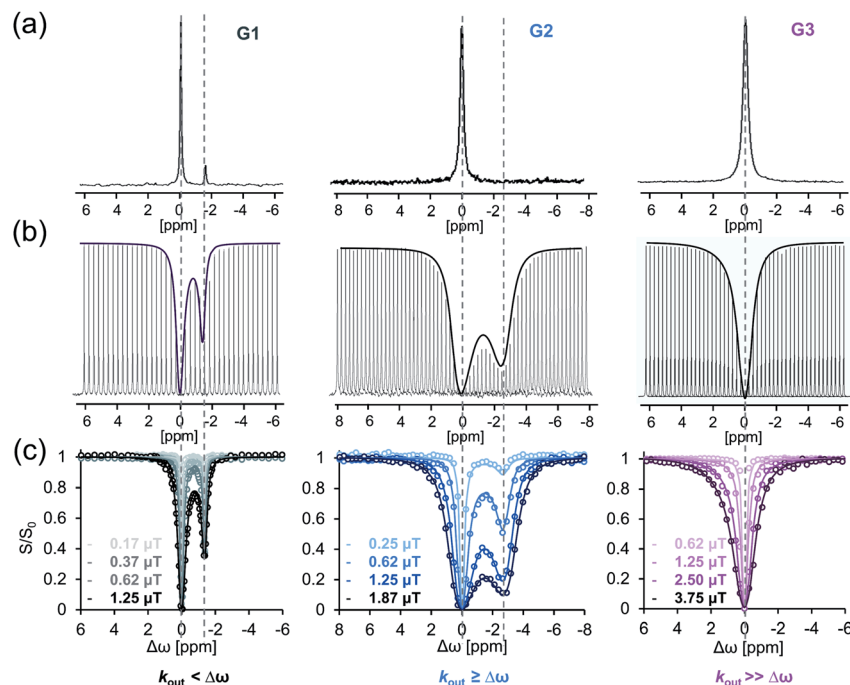


Fig. 2 ^{19}F -NMR and GEST-NMR of the CB7:G systems. (a) ^{19}F -NMR spectra and (b) z-spectra of the GEST experiments performed for each CB7:G system in 5 mM phosphate buffer solution (pH = 7). (c) Multi-B₁ GEST NMR experiments acquired for each of the CB7:G solutions with molar ratios of 1 : 20 for CB7:G1, 1 : 25 for CB7:G2 and 1 : 500 for CB7:G3. Circles represent GEST-NMR experimental data, and solid lines, computational fitting to the Bloch–McConnell equations. The ^{19}F -NMR spectra in (a) were obtained from solutions of 1 : 10 CB7:G ratio.

The linear relationship between $\ln(k_{\text{out}})$ and T^{-1} in eqn (1) can be used to evaluate $E_{\text{a,out}}$ values even for host–guest systems that experience fast exchange ($k_{\text{out}} \gg \Delta\omega$) at a given temperature (e.g., for CB7:G3 at 298 K, Fig. 2b, right). This can be achieved by simply performing a series of GEST experiments at lower temperatures where the condition $k_{\text{out}} \leq \Delta\omega$ is fulfilled. Therefore, we conducted GEST-NMR experiments of CB7 with either G2 or G3 in a phosphate buffer solution (5 mM sodium phosphate, pH = 7) at different temperatures (Fig. 3a, b, S6 and S7†), from which different k_{out} values were extracted and plotted as a function of T^{-1} (Fig. 3c). The obtained linear relationships allowed the estimation of the dissociation E_{a} values (eqn (1)) from the slope of these plots.

Our findings clearly demonstrate that the $E_{\text{a,out}}$ value of CB7:G2 ($53 \pm 1 \text{ kJ mol}^{-1}$) is much higher than that of CB7:G3 ($E_{\text{a,out}} = 32 \pm 1 \text{ kJ mol}^{-1}$), which is in good correlation with the observed differences in the extracted k_{out} values. In comparison, dissociation activation energies of the fluorescent guest berberine and other fluorescent alkaloids are much larger, i.e. $E_{\text{a,out}} > 65 \pm 1 \text{ kJ mol}^{-1}$,⁵⁸ as was determined by direct binding assays. Neither faster equilibrating guests for CB7 with lower $E_{\text{a,out}}$ barriers nor non-chromophoric guests can be investigated by established stopped-flow-coupled direct binding assays. Indeed, we thoroughly attempted to obtain the binding kinetics and activation energies for the CB7:G3 complex by fluorescent-based stopped-flow measurements at a range of different temperatures, pH and salt concentrations. However, in all cases the low emission signal change upon binding and the very fast guest inclusion kinetics prevented the extraction of any

meaningful data with this established protocol. Likewise, even with the newly introduced kinetic versions of the indicator- and guest-displacement assays (*kinGDA* and *kinIDA*) that are applicable also to non-chromophoric guest,⁵⁹ we did not succeed in fitting reliable rate constants for these fast equilibrating guests (Fig. S3–S5†).

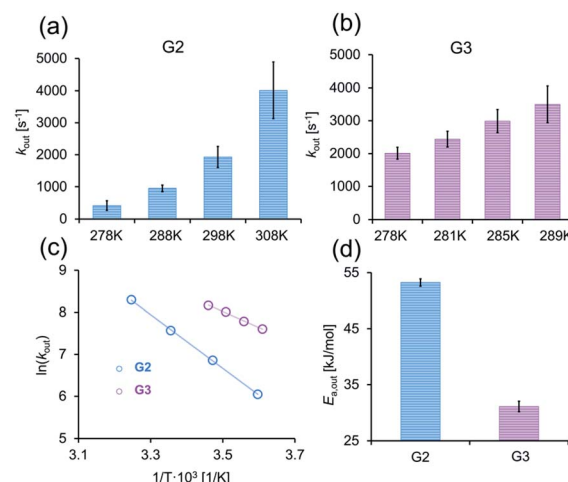


Fig. 3 Dissociation activation energies in CB7:G systems. The dissociation exchange rates (k_{out} , s⁻¹), calculated from GEST-NMR at a series of temperatures, of (a) CB7:G2 and (b) CB7:G3 in 5 mM phosphate buffer. (c) Arrhenius plots of $\ln(k_{\text{out}})$ as a function of the inverse temperature for CB7:G2 and CB7:G3. (d) The calculated $E_{\text{a,out}}$ values for each CB7:G system. CB7:G solutions with molar ratios of 1 : 50 for CB7:G2 and 1 : 100 for CB7:G3 were used.

These results show that by applying GEST-NMR on supramolecular systems with fast exchange dynamic, one can directly quantify $E_{a,out}$ values, providing for the first time access to activation energies of host-guest systems with fast formation and dissociation kinetics. It is important to mention, that CEST-based approaches are less suited for systems with a slow exchange dynamic. In this regard, the slow k_{out} of G1 at 298 K and its relatively low boiling temperature prevented us from performing GEST at higher temperatures to obtain faster k_{out} and thus did not allow to accurately evaluating the $E_{a,out}$ value of CB7:G1.

To investigate GEST-NMR's applicability to systems where the $E_{a,out}$ is mediated also by external factors, we utilized the "supramolecular-lidging" capabilities of monovalent cations known to increase the binding affinities of guests to CB7 in systems with very slow k_{out} characteristics.^{31,53,60,61} As a first step, we used GEST-NMR to determine and quantify the effect of different monovalent cations on the k_{out} of the studied CB7:G3 system (Fig. 4). In contrast to the very fast k_{out} of G3 from its CB7:G3 complex and no asymmetry in the z-spectrum in phosphate buffer solution (Fig. 2b right, 298 K), an increase in the salt concentration resulted in a significant observable asymmetry of the z-spectrum plot. Altering the added cation (*i.e.*, 140 mM of Li^+ , Na^+ , K^+ , Rb^+ , Cs^+ or NH_4^+) resulted in different z-spectrum profiles (Fig. 4a–c and S8†), indicating different k_{out} values (Fig. 4d). Specifically, fitting of the experimental GEST data revealed that the fastest dissociation rate constant occurred in the presence of Li^+ ($k_{out} = 2800 \pm 300 \text{ s}^{-1}$, at 298 K), and the slowest one, in the presence of Na^+ ($k_{out} = 1300 \pm 100 \text{ s}^{-1}$, at 298 K), with an intermediate k_{out} value in the presence of Rb^+ ($k_{out} = 2000 \pm 150 \text{ s}^{-1}$, at 298 K). The reproducibility of this observation was examined and the difference

between the evaluated k_{out} values was found to be statistically significant (Fig. S9†). Note here, that this effect and the obtained dissociation rates were not affected by changes in the pH (Fig. S10†), with similar k_{out} values extracted for the same Na^+ containing solution but with a variety of pH values, *i.e.*, pH = 3 ($1100 \pm 80 \text{ s}^{-1}$), pH = 5 ($1300 \pm 80 \text{ s}^{-1}$), and pH = 7.2 ($1300 \pm 100 \text{ s}^{-1}$). This observation indicates that the dissociation process of the guest from the CB7 cavity is governed primarily by the cation content in the system. To validate that the obtained exchange process is indeed between bound (CB7:G3) and free G3 in solution, a guest that strongly binds to CB7 (*i.e.*, 1-aminoadamantane) was used as a competitor (Fig. S11†). The preferable binding of 1-aminoadamantane to CB7 completely eliminates the GEST effect, confirming that the observed exchange dynamics depend on the availability of the CB7 cavity to accommodate G3. After determining various cation effects on the k_{out} rates in the fast exchanging system CB7:G3 (Fig. 4), we turned to study their effect on the $E_{a,out}$ values.

To this end, we performed GEST-NMR experiments at different temperatures (Fig. 5a and S12†) on CB7:G3 in 5 mM phosphate buffer solution to which LiCl (fast exchange, Fig. 4a), RbCl (intermediate exchange, Fig. 4c) or NaCl (slow exchange, Fig. 4b) was added. The obtained $E_{a,out}$ values (evaluated from the slopes of the linear plots in Fig. 5b) are shown in Fig. 5c. We found that the $E_{a,out}$ value, which was found to be $32 \pm 1 \text{ kJ mol}^{-1}$ in the absence of cations (Fig. 3d), increased in the presence of Li^+ , Rb^+ and Na^+ to 34 ± 2 , 37 ± 5 and $42 \pm 3 \text{ kJ mol}^{-1}$, respectively (Fig. 5c). This observed dependency of the dissociation activation energy for guest exclusion on the

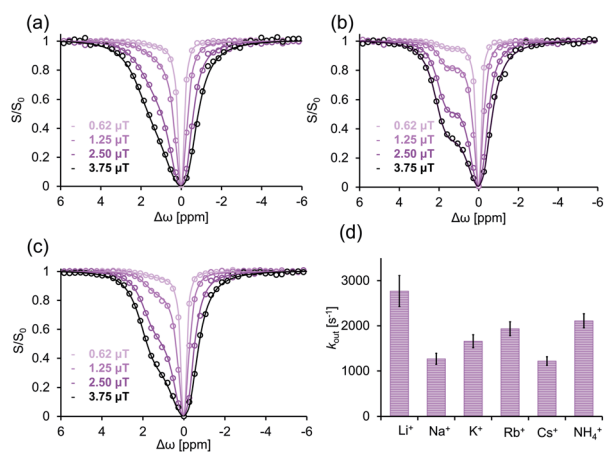


Fig. 4 The effect of cations on fast dissociation exchange rates. Multi- B_1 GEST NMR experiments of CB7:G3 performed at 298 K in 5 mM phosphate buffer under the addition of 140 mM (a) LiCl, (b) NaCl or (c) RbCl. Circles represent GEST-NMR experimental data; solid lines represent fitting curves received by fitting with the Bloch–McConnell equations. (d) k_{out} values of CB7:G3 in the presence of various monovalent cations. CB7:G3 solutions at 1 : 500 ratio were prepared in 5 mM phosphate buffer (pH = 7) under the addition of 140 mM of MCl ($M = Li^+, Na^+, K^+, Rb^+, Cs^+, NH_4^+$).

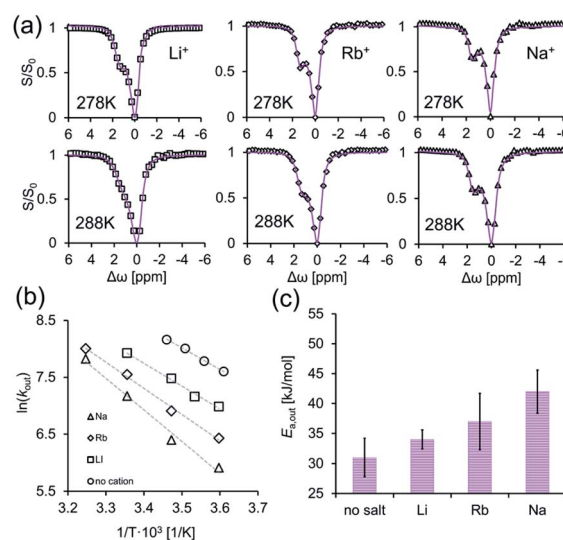


Fig. 5 Dissociation rate as a function of monovalent cations. Dissociation activation energy as a function of monovalent cations. (a) Experimental z-spectra of GEST experiments performed at different temperatures (278 K and 288 K) for CB7:G3 in a 5 mM phosphate buffer solution to which 140 mM LiCl (left), 140 mM RbCl (middle), or 140 mM NaCl (right) was added; (b) Plots of $\ln(k_{out})$ as function of the inverse temperature for CB7:G3 (1 : 500 ratio) in 5 mM phosphate buffer solution in the presence or absence of 140 mM LiCl, RbCl or NaCl. (c) Evaluation of the dissociation E_a values from the slopes of the plots shown in (b).

cationic content manifests its role in mediating the dissociation process even in systems with fast exchange kinetics. By combining $E_{a,\text{out}}$ values with the enthalpy change of the reaction (extracted from the ITC data for each system, Fig. S13†), the association activation energy ($E_{a,\text{in}}$) values were accessible. Furthermore, assuming a one-step reaction, we used the correlation of the Eyring equation to calculate the dissociation activation free energy ($\Delta G_{\text{out}}^\ddagger$) as summarized in Table 1.

To confirm the formation of supramolecular CB7 “capsules” with $\text{M}^+ \cdot \text{CB7} \cdot \text{G3} \cdot \text{M}^+$ and to assure that $\text{M}^+ \cdot \text{CB7}$ capping indeed occurred and mediated the obtained $E_{a,\text{out}}$ values, 1D-NMR (^7Li -NMR, ^{23}Na -NMR and ^{87}Rb -NMR) and ^7Li - and ^{23}Na -diffusion NMR experiments were performed.^{62,63} This entailed the direct measurement of the NMR-characteristics of the cations (Li^+ , Na^+ or Rb^+) in aqueous solutions of LiCl, NaCl and RbCl with and without CB7. From the obtained 1D ^7Li -NMR, ^{23}Na -NMR and ^{87}Rb -NMR spectra, it is evident that CB7 has no effect on the chemical shift of $^7\text{Li}^+$ (Fig. 6a, left), which is in contrast to the pronounced effect on the chemical shift of $^{23}\text{Na}^+$ (Fig. 6a, middle) and $^{87}\text{Rb}^+$ (Fig. 6a, right).

These observations indicate a stronger interaction of CB7 with the Rb^+ and Na^+ cations as compared to that with the Li^+ cations and correlate with previous studies showing that different cations have different affinities to the portals of CBns.^{47,52,60,61,64–67} Our ^7Li - and ^{23}Na -diffusion NMR experiments are in agreement with previous reports⁶⁸ and further corroborate these observation (Fig. 6b). Notably, we found no significant change in the diffusion coefficient of Li^+ upon the addition of CB7, further corroborating that this cation does not bind to the portals of the host (Fig. 6b, left). In contrast, we noted a significant reduction in the diffusion coefficient of Na^+ upon the addition of the CB7 host, either with or without G3 (Fig. 6b, right). The shift in the ^{133}Cs -NMR spectrum (Fig. S14a†) and the decrease in the diffusion coefficient of $^{133}\text{Cs}^+$ in the presence of CB7 (Fig. S14b†) were similar to those obtained for Na^+ . This correlates with the slowest and similar k_{out} values calculated for CB7:G3 in the presence of either Na^+ or Cs^+ (Fig. 4d). Such a reduction in Na^+ (or Cs^+ , Fig. S14b†) diffusivity confirms that these cations strongly bind to the CB7 portals and serve as an active “lid”, in comparison to the in size smaller Li^+ cation. These observed different affinities of various cations to the host portals govern the changes in the transition energy barrier of the host–guest complex and, therefore, mediate guest egression kinetics.⁶¹

Table 1 Kinetic parameters calculated for CB7:G3 dissolved in 5 mM phosphate buffer under the addition of different cations (LiCl, RbCl, NaCl, $c = 140 \text{ mM}$ each)

	CB7:G3 + Li^+	CB7:G3 + Rb^+	CB7:G3 + Na^+
$k_{\text{out}} [\text{s}^{-1}] (T = 298 \text{ K})$	2800 ± 300	2000 ± 150	1300 ± 100
$E_{a,\text{out}} [\text{kJ mol}^{-1}]$	34 ± 2	37 ± 5	42 ± 3
$E_{a,\text{in}} [\text{kJ mol}^{-1}]$	15 ± 2	17 ± 5	33 ± 3
$\Delta H_{\text{out}}^\ddagger [\text{kJ mol}^{-1}]$	36 ± 2	40 ± 5	45 ± 3
$T\Delta S_{\text{out}}^\ddagger [\text{kJ mol}^{-1}]$	-22 ± 1	-20 ± 5	-16 ± 4
$\Delta G_{\text{out}}^\ddagger [\text{kJ mol}^{-1}]^a$	58 ± 1	59 ± 4	60 ± 3

^a Calculated using the Eyring equation.

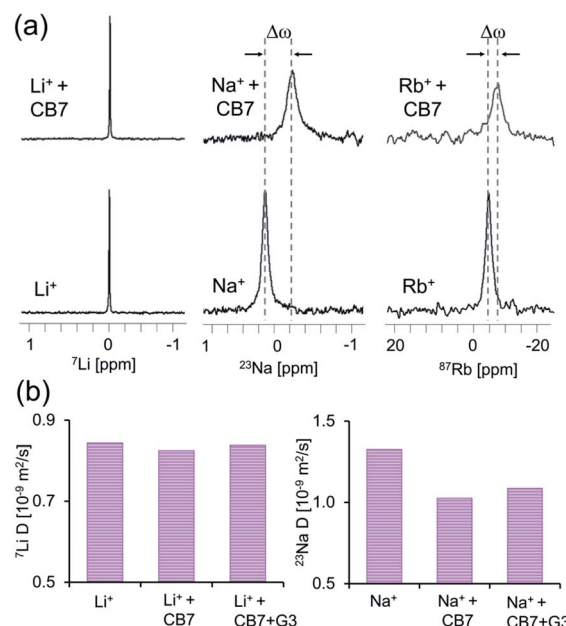


Fig. 6 NMR studies of cations binding to CB7. (a) ^7Li -NMR, ^{87}Rb -NMR and ^{23}Na -NMR with (upper) and without (lower) CB7. (b) ^7Li - and ^{23}Na -diffusion coefficients in phosphate buffer solutions containing free M^+ , $\text{M}^+ \cdot \text{CB7}$, and $\text{M}^+ \cdot \text{CB7} \cdot \text{G3}$. Ratios of 1 : 4 CB7: M^+ and 1 : 2 of CB7:G3 were used with 2 mM CB7.

Conclusions

In summary, GEST-NMR was used to elucidate dissociation activation energies in host–guest assemblies featuring fast exchange dynamics highlighting the role of “supramolecular lids” in mediating guests’ dissociation E_a . Our results emphasize GEST’s ability to quantify exchange rates that cannot be measured by other approaches used for the study of kinetics in host–guest systems, in general, and in particular in CBn–guest systems.^{31,53,69,70} Performing GEST-NMR at a range of temperatures and plotting the quantified k_{out} values as a function of the (inverse) experimental temperature allowed the evaluation of different dissociation activation energies with various kinetic profiles. Finally, we demonstrated the role of monovalent cations in mediating k_{out} and the energetic barrier of guest dissociation by their supramolecular capping features for a fast-exchanging system. Thus, GEST can serve as an important analytical tool in designing supramolecular systems where controlling the E_a is crucial, such as switchable molecular host systems.^{9–11} The fact that GEST can be applied with a conventional NMR setup, which is available at any research institute, offers new opportunities to explore dissociation dynamics and E_a in a variety of supramolecular systems and should provide insights into less-studied mechanisms. The extension of CEST-NMR experiments to ^{15}N - and ^{13}C - and its implementation in other dynamic molecular systems, such as proteins,^{71,72} emphasizes the potential of the proposed approach to be further developed. Because state-of-the-art experimental methods for determining the rate constants of host–guest complexes were so far limited to comparably slow binding



systems ($<10\text{ s}^{-1}$), having now a method at avail that can also be applied to rapidly unbinding guests ($>1000\text{ s}^{-1}$) may open new possibilities for shedding light on fundamental questions in host-guest complexation kinetics. GEST can thus provide an additional insight into binding mechanisms in host-guest systems, as for example in the influence of guest and host desolvation that remains hidden so far. Therefore, we envision that using GEST-NMR for the study of binding kinetics and dissociation E_a will advance the knowledge of supramolecular systems toward better understanding their kinetic properties and allow their further development as functional materials.

Conflicts of interest

There are no conflicts to declare.

Acknowledgements

This project has received funding from the European Research Council (ERC) under the European Union's Horizon 2020 research and innovation programme (grant agreement No 677715). We thank Dr Moritz Zaiss from the Max Planck Institute for Biological Cybernetics for providing the CEST data-fitting tool and consultations.

Notes and references

- 1 R. Wang, Y. Sun, F. Zhang, M. Song, D. Tian and H. Li, *Angew. Chem., Int. Ed.*, 2017, **56**, 5294–5298.
- 2 Z. Rodriguez-Docampo, S. I. Pascu, S. Kubik and S. Otto, *J. Am. Chem. Soc.*, 2006, **128**, 11206–11210.
- 3 S. Peng, A. Barba-Bon, Y. C. Pan, W. M. Nau, D. S. Guo and A. Hennig, *Angew. Chem., Int. Ed.*, 2017, **56**, 15742–15745.
- 4 Q. Duan, Y. Cao, Y. Li, X. Hu, T. Xiao, C. Lin, Y. Pan and L. Wang, *J. Am. Chem. Soc.*, 2013, **135**, 10542–10549.
- 5 S. R. Shenoy, F. R. Pinacho Crisostomo, T. Iwasawa and J. Rebek Jr, *J. Am. Chem. Soc.*, 2008, **130**, 5658–5659.
- 6 E. A. Appel, J. del Barrio, X. J. Loh and O. A. Scherman, *Chem. Soc. Rev.*, 2012, **41**, 6195–6214.
- 7 X. Yan, F. Wang, B. Zheng and F. Huang, *Chem. Soc. Rev.*, 2012, **41**, 6042–6065.
- 8 A. K. Chan, W. H. Lam, Y. Tanaka, K. M. Wong and V. W. Yam, *Proc. Natl. Acad. Sci. U. S. A.*, 2015, **112**, 690–695.
- 9 D. H. Qu, Q. C. Wang, Q. W. Zhang, X. Ma and H. Tian, *Chem. Rev.*, 2015, **115**, 7543–7588.
- 10 Y. Liu, A. H. Flood and J. F. Stoddart, *J. Am. Chem. Soc.*, 2004, **126**, 9150–9151.
- 11 I. Pochorovski and F. Diederich, *Acc. Chem. Res.*, 2014, **47**, 2096–2105.
- 12 Z. Miskolczy, L. Biczok and I. Jablonkai, *Phys. Chem. Chem. Phys.*, 2016, **19**, 766–773.
- 13 S. Sánchez Carrera, J.-L. Kerdelhué, K. J. Langenwalter, N. Brown and R. Warmuth, *Eur. J. Org. Chem.*, 2005, **2005**, 2239–2249.
- 14 T. Brotin and J.-P. Dutasta, *Eur. J. Org. Chem.*, 2003, **2003**, 973–984.
- 15 L. Schroder, T. J. Lowery, C. Hilty, D. E. Wemmer and A. Pines, *Science*, 2006, **314**, 446–449.
- 16 Y. Bai, P. A. Hill and I. J. Dmochowski, *Anal. Chem.*, 2012, **84**, 9935–9941.
- 17 M. Kunth, J. Dopfert, C. Witte, F. Rossella and L. Schroder, *Angew. Chem., Int. Ed.*, 2012, **51**, 8217–8220.
- 18 M. Kunth, C. Witte, A. Hennig and L. Schroder, *Chem. Sci.*, 2015, **6**, 6069–6075.
- 19 M. Schnurr, J. Sloniec-Myszk, J. Dopfert, L. Schroder and A. Hennig, *Angew. Chem., Int. Ed.*, 2015, **54**, 13444–13447.
- 20 Y. Wang and I. J. Dmochowski, *Chem. Commun.*, 2015, **51**, 8982–8985.
- 21 M. Schnurr, R. Joseph, A. Naugolny-Keisar, D. Kaizerman-Kane, N. Bogdanoff, P. Schuenke, Y. Cohen and L. Schroder, *ChemPhysChem*, 2019, **20**, 246–251.
- 22 K. Du, S. D. Zemerov, S. Hurtado Parra, J. M. Kikkawa and I. J. Dmochowski, *Inorg. Chem.*, 2020, **59**, 13831–13844.
- 23 Y. Wang and I. J. Dmochowski, *Acc. Chem. Res.*, 2016, **49**, 2179–2187.
- 24 A. Bar-Shir, A. A. Gilad, K. W. Chan, G. Liu, P. C. van Zijl, J. W. Bulte and M. T. McMahon, *J. Am. Chem. Soc.*, 2013, **135**, 12164–12167.
- 25 A. Bar-Shir, N. N. Yadav, A. A. Gilad, P. C. van Zijl, M. T. McMahon and J. W. Bulte, *J. Am. Chem. Soc.*, 2015, **137**, 78–81.
- 26 L. Avram, V. Havel, R. Shusterman-Krush, M. A. Iron, M. Zaiss, V. Sindelar and A. Bar-Shir, *Chem.-Eur. J.*, 2019, **25**, 1687–1690.
- 27 L. Avram, M. A. Iron and A. Bar-Shir, *Chem. Sci.*, 2016, **7**, 6905–6909.
- 28 L. Avram, A. D. Wishard, B. C. Gibb and A. Bar-Shir, *Angew. Chem., Int. Ed.*, 2017, **56**, 15314–15318.
- 29 L. Avram and A. Bar-Shir, *Org. Chem. Front.*, 2019, **6**, 1503–1512.
- 30 M. Megyesi, L. Biczók and I. Jablonkai, *J. Phys. Chem. C*, 2008, **112**, 3410–3416.
- 31 H. Tang, D. Fuentealba, Y. H. Ko, N. Selvapalam, K. Kim and C. Bohne, *J. Am. Chem. Soc.*, 2011, **133**, 20623–20633.
- 32 E. A. Appel, F. Biedermann, D. Hoogland, J. Del Barrio, M. D. Driscoll, S. Hay, D. J. Wales and O. A. Scherman, *J. Am. Chem. Soc.*, 2017, **139**, 12985–12993.
- 33 E. Masson, M. Ræisi and K. Kotturi, *Isr. J. Chem.*, 2018, **58**, 413–434.
- 34 Z. Miskolczy and L. Biczok, *J. Phys. Chem. B*, 2014, **118**, 2499–2505.
- 35 C. Bohne, *Chem. Soc. Rev.*, 2014, **43**, 4037–4050.
- 36 M. D. Pluth and K. N. Raymond, *Chem. Soc. Rev.*, 2007, **36**, 161–171.
- 37 C. L. Perrin and T. J. Dwyer, *Chem. Rev.*, 1990, **90**, 935–967.
- 38 J. Lagona, P. Mukhopadhyay, S. Chakrabarti and L. Isaacs, *Angew. Chem., Int. Ed.*, 2005, **44**, 4844–4870.
- 39 S. J. Barrow, S. Kasera, M. J. Rowland, J. del Barrio and O. A. Scherman, *Chem. Rev.*, 2015, **115**, 12320–12406.
- 40 D. Shetty, J. K. Khedkar, K. M. Park and K. Kim, *Chem. Soc. Rev.*, 2015, **44**, 8747–8761.
- 41 K. I. Assaf and W. M. Nau, *Chem. Soc. Rev.*, 2015, **44**, 394–418.



- 42 D. W. Lee, K. M. Park, M. Banerjee, S. H. Ha, T. Lee, K. Suh, S. Paul, H. Jung, J. Kim, N. Selvapalam, S. H. Ryu and K. Kim, *Nat. Chem.*, 2011, **3**, 154–159.
- 43 Z. Hirani, H. F. Taylor, E. F. Babcock, A. T. Bockus, C. D. Varnado Jr, C. W. Bielawski and A. R. Urbach, *J. Am. Chem. Soc.*, 2018, **140**, 12263–12269.
- 44 S. K. Samanta, J. Quigley, B. Vinciguerra, V. Briken and L. Isaacs, *J. Am. Chem. Soc.*, 2017, **139**, 9066–9074.
- 45 A. I. Lazar, F. Biedermann, K. R. Mustafina, K. I. Assaf, A. Hennig and W. M. Nau, *J. Am. Chem. Soc.*, 2016, **138**, 13022–13029.
- 46 A. Palma, M. Artelsmair, G. Wu, X. Lu, S. J. Barrow, N. Uddin, E. Rosta, E. Masson and O. A. Scherman, *Angew. Chem., Int. Ed.*, 2017, **56**, 15688–15692.
- 47 S. Zhang, L. Grimm, Z. Miskolczy, L. Biczok, F. Biedermann and W. M. Nau, *Chem. Commun.*, 2019, **55**, 14131–14134.
- 48 A. L. Koner, C. Marquez, M. H. Dickman and W. M. Nau, *Angew. Chem., Int. Ed.*, 2011, **50**, 545–548.
- 49 K. A. Kellersberger, J. D. Anderson, S. M. Ward, K. E. Krakowiak and D. V. Dearden, *J. Am. Chem. Soc.*, 2001, **123**, 11316–11317.
- 50 Y. Miyahara, K. Abe and T. Inazu, *Angew. Chem., Int. Ed.*, 2002, **41**, 3020–3023.
- 51 S. He, F. Biedermann, N. Vankova, L. Zhechkov, T. Heine, R. E. Hoffman, A. De Simone, T. T. Duignan and W. M. Nau, *Nat. Chem.*, 2018, **10**, 1252–1257.
- 52 W. Ong and A. E. Kaifer, *J. Org. Chem.*, 2004, **69**, 1383–1385.
- 53 S. S. Thomas, H. Tang and C. Bohne, *J. Am. Chem. Soc.*, 2019, **141**, 9645–9654.
- 54 Z. Miskolczy, M. Megyesi, L. Biczok, A. Prabodh and F. Biedermann, *Chem.–Eur. J.*, 2020, **26**, 7433–7441.
- 55 M. Zaiss, G. Angelovski, E. Demetriou, M. T. McMahon, X. Golay and K. Scheffler, *Magn. Reson. Med.*, 2018, **79**, 1708–1721.
- 56 L. Perez, B. G. Caulkins, M. Mettry, L. J. Mueller and R. J. Hooley, *Chem. Sci.*, 2018, **9**, 1836–1845.
- 57 P. C. van Zijl and N. N. Yadav, *Magn. Reson. Med.*, 2011, **65**, 927–948.
- 58 Z. Miskolczy, M. Megyesi, O. Toke and L. Biczok, *Phys. Chem. Chem. Phys.*, 2019, **21**, 4912–4919.
- 59 A. Prabodh, S. Sinn, L. Grimm, Z. Miskolczy, M. Megyesi, L. Biczok, S. Brase and F. Biedermann, *Chem. Commun.*, 2020, **56**, 12327–12330.
- 60 Y.-M. Jeon, J. Kim, D. Whang and K. Kim, *J. Am. Chem. Soc.*, 1996, **118**, 9790–9791.
- 61 C. Marquez, R. R. Hudgins and W. M. Nau, *J. Am. Chem. Soc.*, 2004, **126**, 5806–5816.
- 62 L. Avram and Y. Cohen, *Chem. Soc. Rev.*, 2015, **44**, 586–602.
- 63 Y. Cohen, L. Avram and L. Frish, *Angew. Chem., Int. Ed.*, 2005, **44**, 520–554.
- 64 M. Morisue, S. Ueda, M. Kurasawa, M. Naito and Y. Kuroda, *J. Phys. Chem. A*, 2012, **116**, 5139–5144.
- 65 H.-J. Buschmann, E. Cleve, L. Mutihac and E. Schollmeyer, *J. Inclusion Phenom. Macrocyclic Chem.*, 2009, **65**, 293.
- 66 X. Shi, W. Gu, C. Zhang, L. Zhao, L. Li, W. Peng and Y. Xian, *Chem.–Eur. J.*, 2016, **22**, 5643–5648.
- 67 L. L. Liang, X. L. Ni, Y. Zhao, K. Chen, X. Xiao, Y. Q. Zhang, C. Redshaw, Q. J. Zhu, S. F. Xue and Z. Tao, *Inorg. Chem.*, 2013, **52**, 1909–1915.
- 68 N. J. Wheate, P. G. Kumar, A. M. Torres, J. R. Aldrich-Wright and W. S. Price, *J. Phys. Chem. B*, 2008, **112**, 2311–2314.
- 69 A. Hennig, H. Bakirci and W. M. Nau, *Nat. Methods*, 2007, **4**, 629–632.
- 70 F. Biedermann and W. M. Nau, *Angew. Chem., Int. Ed.*, 2014, **53**, 5694–5699.
- 71 G. Bouvignies and L. E. Kay, *J. Biomol. NMR*, 2012, **53**, 303–310.
- 72 V. P. Tiwari, S. Pandit and P. Vallurupalli, *J. Biomol. NMR*, 2019, **73**, 43–48.

